Nanoscale

Accepted Manuscript

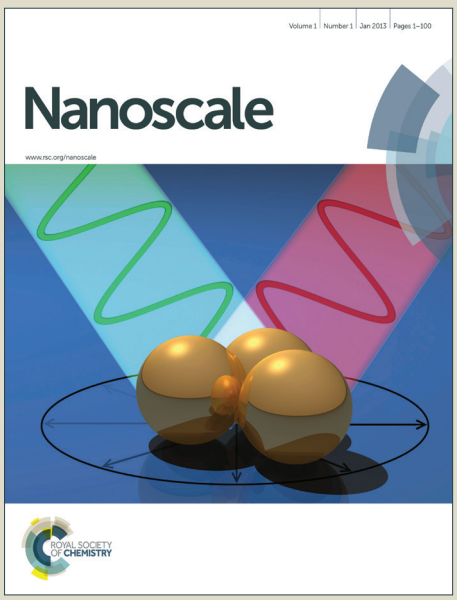

This is an *Accepted Manuscript*, which has been through the Royal Society of Chemistry peer review process and has been accepted for publication.

Accepted Manuscripts are published online shortly after acceptance, before technical editing, formatting and proof reading. Using this free service, authors can make their results available to the community, in citable form, before we publish the edited article. We will replace this *Accepted Manuscript* with the edited and formatted *Advance Article* as soon as it is available.

You can find more information about *Accepted Manuscripts* in the Information for Authors.

Please note that technical editing may introduce minor changes to the text and/or graphics, which may alter content. The journal's standard Terms & Conditions and the Ethical guidelines still apply. In no event shall the Royal Society of Chemistry be held responsible for any errors or omissions in this *Accepted Manuscript* or any consequences arising from the use of any information it contains.

ROYAL SOCIETY OF CHEMISTRY

www.rsc.org/nanoscale

Cite this: DOI: 10.1039/c0xx00000x

www.rsc.org/xxxxxx

ARTICLE TYPE

From Basic Physics to Mechanisms of Toxicity: "Liquid Drop" Approach Applied to Develop Predictive Classification Models for Toxicity of Metal Oxide Nanoparticles

Natalia Novoselska,[a,b] Bakhtiyor Rasulev,[b] Agnieszka Gajewicz,[c] Victor Kuz'min,[a,d] Tomasz Puzyn[c] and JerzyLeszczynski*[b]

Received (in XXX, XXX) Xth XXXXXXXXX 20XX, Accepted Xth XXXXXXXXX 20XX
DOI: 10.1039/b000000x

Many metal oxide nanoparticles are able to cause persistent stress to live organisms, including humans, when discharged to environment. To understand the mechanism of metal oxides nanoparticles toxicity and reduce a number of experiments the development of predictive toxicity models is important. In this study, performed on a series of nanoparticles, the comparative Quantitative-Structure Activity Relationships (nano-QSARs) analyses of their toxicity towards *E.coli* and *HaCaT* cells were established. A new approach for representation of nanoparticles' structure was presented. For description of supramolecular structure of nanoparticles "liquid drop" model was applied. It is expected that novel, proposed approach could be of general use for predictions related to nanomaterials. In addition, in our study fragmental simplex descriptors and several ligand-metal binding characteristics were calculated. The developed nano-QSAR models were validated and reliably predict toxicity of all studied metal oxide nanoparticles. Based on the comparative analysis of contributed properties in both models the LDM-based descriptors were revealed to have almost similar level of contribution to toxicity in both cases, while other parameters (van-der-Waals interactions, electronegativity and metal-ligand binding characteristics) have unequal contribution levels. In addition, the models developed here suggest different mechanisms of nanotoxicity for these two types of cells.

Nanoscale Accepted Manuscript

Cite this: DOI: 10.1039/c0xx00000x

www.rsc.org/xxxxxx

ARTICLE TYPE

Introduction

A group of metal oxide nanoparticles represents one of the most remarkable nanomaterials because of their outstanding magnetic, mechanical, catalytic, electronic, semiconducting and various other properties. Such properties depend greatly on nanoparticle's size, structure, and shape and make them valuable components for broad range of applications, including industrial, medical, chemical, and scientific. Conservative market evaluated the production for metal oxide nanoparticles in 2012 at about 270,041 tons, likely rising to 1,663,168 tons by 2020[1].

Most of the metal oxide nanoparticles are persistent and able to cause persistent stress to live organisms, including humans, when exposed to environment[2-4]. Since metal oxides in nano-sizes exhibit peculiar physico-chemical properties that make them dramatically different from bulk-sized forms these nanomaterials were subjected extensively to various experimental studies, including environmental and toxicological[4, 5].

To reduce a number of experiments and reveal the mechanism of nano-sized metal oxides toxicity the combined experimental and computational modeling studies were performed by different research groups, resulting in development of various predictive models[4-20]. For example, the mathematical model based on quantum-chemically calculated descriptors to predict cytotoxicity of nano-sized metal oxides was recently reported[6]. In another study a QSAR model was built to predict cellular uptake for a series of nanoparticles separating the organic part (surface modifier) from the common core (metal and metal oxide core)[7]. Interesting study was performed by Zhang et al[18] where authors were able to find a correlation between band gap and cytotoxicity. They also performed oxidative stress assays tests for series of metal oxide nanoparticles. Burello and Worth[16] suggested similar band gap descriptor to estimate oxidative stress ability of metal oxides based on 6 metal oxides and utilized developed model to predict oxidative stress ability for another 64 hypothetical metal oxide nanoparticles.

For the last decade nanotoxicologists proposed several different mechanisms by which nanoparticles interact with cell systems and penetrate into microorganisms or cells[6, 16, 19, 21-30]. For example, some nanoparticles can penetrate into test-systems with no specific receptors on their outer surface. This uptake may be initiated by van-der-Waals forces, electrostatic charges and steric interactions (size, geometries, bonding)[2]. To describe this type of interactions various theoretical methods could be used, including quantum-chemical calculations (QC), empirical formulas and approaches/software commonly used to calculate theoretical descriptors, like ChemAxon[31], Dragon[32], CDK[33], and SiRMS (Simplex Representation of Molecular Structure) approach[34] .

Based on our experience with predictive QSAR modeling and especially with nanoparticles properties prediction[6, 8, 10, 11, 34-43], we suggest that for successful description of properties or mechanisms it is beneficial to use a combination of descriptors which reflect nanoparticles' structure for the different levels of organization: from single molecule to supramolecular ensemble of molecules.

Thus, to simplify the representation of possible interactions on the nano-level in the present work we have utilized a "liquid drop" model (LDM)[44]. This is a very first, innovative study that applies models developed in physics to describe interactions of nanomaterials with biological systems. The study opens a new way of inclusions of several vital characteristics of nanomaterials in general parameters that could be used to uncover complex phenomena of their effects on biomolecules. It is worth to note, that LDM is able to describe such important properties of nanoparticle as surface area, surface to volume ratio, etc. Also LDM-based descriptors are size-dependent, that allows applying them for the series of nanoparticles with same chemical composition, but different sizes. Therefore, we believe that the proposed approach could be of general use for predictions related to nanomaterials.

Besides of some specific interactions of nanoparticle's surface with a target system several studies suggest that the mechanism of nanoparticles' toxicity depends on release of ions from the surface[6, 16, 17, 45]. Also Mathews[46] proposed that ionic forms of metals are more active and explained this fact by the process of ion binding to biomolecules. In this connection Tatara[47] attempted to obtain a QSAR model for toxicity of metal ions using several ion characteristics. In addition, Newman[48] demonstrated that this approach was suitable for toxicity prediction of the same species. Based on this, in the current work we have applied similar ion characteristics to reflect the ability of metal ions to interact with membranes.

In summary, in the present study the new approaches were applied to perform a comparative analysis of the QSAR models based on metal oxide nanoparticles' cytotoxicity to bacteria *Escherichia coli* (prokaryotic cells) and *HaCaT* cells (eukaryotic cells).

Materials and Methods

Biological activity data

The toxicity data for nano-sized metal oxides against *E.coli* and *HaCaT* cells were analyzed and all original experimental data were taken from our previous publications[6, 49]. Datasets consist of 17 and 18 metal oxide nanoparticles well characterized and then tested against *E.coli* and *HaCaT* cells, respectively. Originally measured *in vitro* effective concentration EC_{50} toxicity data (mol/L) were expressed as logarithm of the inverse molar concentration ($\log(1/EC_{50})$) response variables. The structures, investigated toxicity values and sizes of individual nanoparticles and aggregation sizes are given in Table 1.

Computational Details

The main idea of proposed here approach was to use a combination of simple descriptors which reflect nanoparticles' structure for the different levels of organization: from single metal oxide molecule (i.e. chemical structure) to supramolecular ensemble of molecules (i.e. nanoparticle size). To characterize a single metal oxide structure at the 2D level a Simplex Representation of Molecular Structure (SiRMS)[34] methodology was used. To simplify the representation of possible interactions at the nano-level without

Nanoscale Accepted Manuscript

quantum-chemical modeling the "liquid drop" model (LDM)[44] was utilized. In addition, the properties of single metal cations were expressed using Metal-ligand binding (MLB) theory. When applying these steps, extensive quantum-mechanical calculations for relatively large (from computational pointer view) molecular clusters might be avoided.

Simplex Representations of Molecular Structure

The SiRMS (Simplex Representation of Molecular Structure) approach was used to encode the first level of organization of investigated objects. In the framework of SiRMS, any molecule (chemical structure) can be represented as a system of different simplexes (fragments of fixed composition and topology)[34]. This approach expands features of other methods of fragment representation, by providing ability to perform the differentiation of atoms in simplex not only by their type, but also based on the different characteristics of atoms (electronegativity, lipophilicity, van-der-Waals interactions, etc).

In the current study we utilized a 2D level of molecule's representation to generate simplex fragments. Initially, a molecule was represented as a molecular graph. All vertices in graph that represent characteristic features of atom, for example type of atom, the connectivity of atoms in graph, and bond nature were considered. Then atoms in molecule were encoded on the basis of various physicochemical properties and subsequently the organization of values' range into definite discrete groups was performed. In this study all values of atoms' differentiation were clustered into groups corresponding to their electronegativity (A<1.5<B<2.0<C<2.5<D<3.5<F) and Lennard-Jones potential (A<0.01<B<0.02<C<0.4<D for depth of the potential well and A<2.5<B<3<C<3.5<D<4<F for distance at which potential reaches minimum). Example of differentiation is shown in Fig.1.

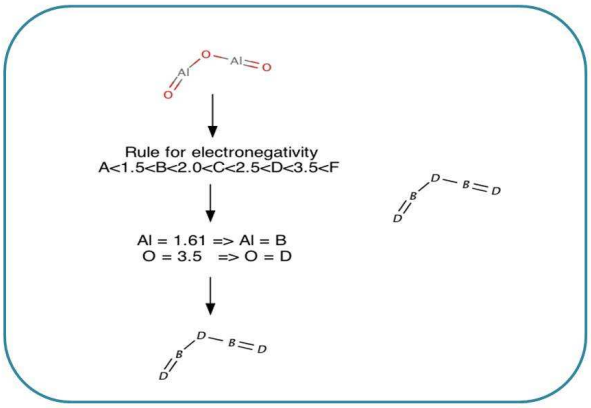

Fig. 1 Example of TiO_2 attribution based on SiRMS differentiation of by electronegativity

Since the electronegativity value of Al_2O_3 is equal to 1.61 and electronegativity of O is 3.5, after differentiation applied based on the above rule the initial molecule Al_2O_3 can be represented as B_2D_3.

After differentiation step molecular graphs were fragmentized to combination of simplexes. As a regular procedure, SiRMS approach utilize molecular fragment size of 2 to 4 atoms, however taking into account that the objects of study are metal oxides, the shorter molecular fragments (1 to 3 atoms) were considered. Example of fragmentization is shown in Fig.2.

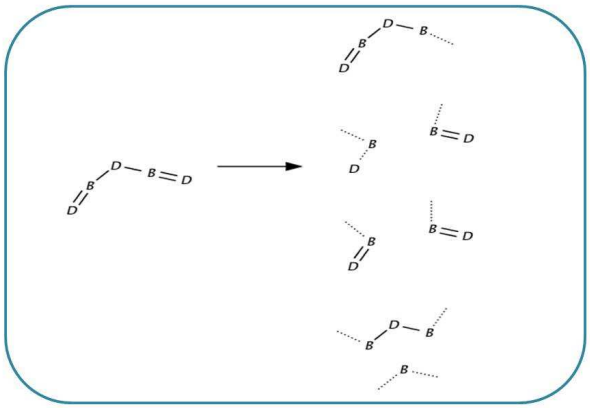

Fig. 2 Example of fragmentization

As a result, the net number of fragments (simplexes) of each type was used as a descriptor in model development.

Liquid Drop Model

Innovative approach is proposed in our study. We have introduced a liquid drop model, LDM, in order to encode the nanoparticle clusters (aggregates) in a solution. In LDM, nanoparticle is represented as a spherical drop, where elementary particles (molecules) are densely packed and density of cluster is equal to mass density[44]. In this model the minimum radius of interactions between elementary particles in cluster is described by Wigner-Seitz radius[50]:

$$r_W = \left(\frac{3M}{4\pi\rho N_A} \right)^{1/3} \quad (1)$$

where M - molecular weight, ρ - mass density, N_A - Avogadro constant.

LDM assumes that the most probable nanoparticles' shape is spherical (as well as shape of nanoparticles' aggregates in water). Based on this assumption the method assumes that the number of molecules in nanocluster is equal to:

$$n = \left(\frac{r_0}{r_W} \right)^3 \quad (2)$$

where r_0 - nanoparticle's radius;

The equation (2) shows that the smaller the particle, the higher the ratio of surface to volume is. In other words, decreasing size of a particle considerably increases its surface area. It distinguishes the nanoparticles' surface molecules from the other molecules in volume. It means that interaction forces between molecules located inside of molecular volume are not compensated by interaction forces of the same molecules located on the surface, i.e. the molecules on the surface are in special circumstances (Fig. 3).

Nanoscale Accepted Manuscript

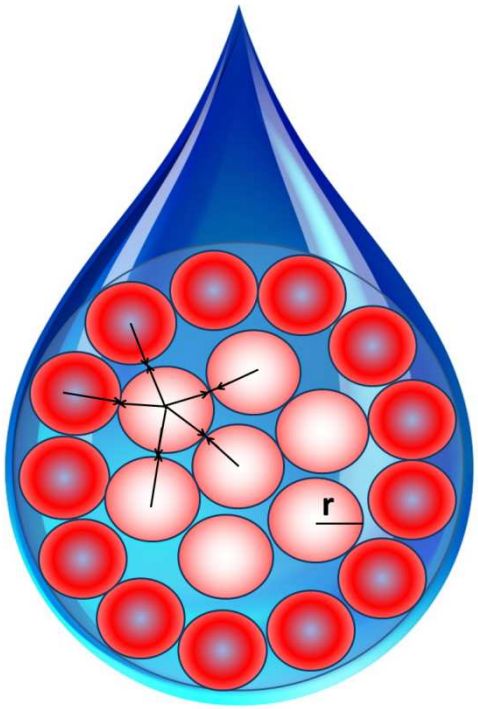

Fig. 3 Liquid drop model of a nanoparticle**.** Interaction forces between molecules located in the volume (white circles); interaction forces of the molecules located on the surface on the nanoparticle (red circles)

Based on that, the ratio of surface molecules (F) to molecules in volume is supposed to be significant:

$$F = 4n^{-1/3} \quad (3)$$

As a result, more specific and more interpretative descriptor *(SV)* is proposed that describes the ratio of surface molecules to molecules in volume:

$$(SV) = \left(\frac{\text{surface molecules}}{\text{molecules in volume}}\right) = \frac{F}{1-F} \quad (4)$$

Aggregation of nanoparticles also plays an important role in estimation of their toxicity[51]. For example, small nanoparticles can localize in organelles in contrary to larger ones. Aggregation parameter *(AP)* reflects ratio of particles in aggregate in comparing to size of single particle:

$$(AP) = \frac{\text{size of aggregate}}{\text{size of single particle}} \quad (5)$$

Metal-Ligand Binding Characteristics

Metal-ligand binding (MLB) theory pre-assumes that binding of metals to soft ligands on biomolecules plays an important role in toxicity exhibition[46].

In the current study two ion characteristics (MLB) were used to describe ability of metal ion's affinity to biochemical ligands: covalent index *(CI)* and cation polarizing power *(CPP)*.

(CI) reflects the relative importance of covalent interactions relative to ionic during metal-ligand binding[37]. For example, this includes interactions with protein-bonded sulfhydryl's or depleting of glutathione. *(CI)* represents combination of the electronegativity (χ) and Pauling radius (r):

$$(CI) = \chi_m^2 r \quad (6)$$

(CPP) encodes the energy of metal ion during electrostatic interaction with a ligand and represents the combination of ion charge (Z) and Pauling radius (r):

$$(CPP) = Z^2/r \quad (7)$$

Model development. Random Forests method

The relationships between measured toxicity and calculated descriptors were established with Random Forest (RF) regression method using the RandomForest package[52].

RF is an ensemble classifier proposed by Breiman[53]. It constructs a series of decision trees which are used to classify a new sample. At the regression process the average of the individual tree predictions of all trees are combined to produce one final prediction. Every node in tree called "decision rule". For example, a decision tree is shown in Fig. 4.

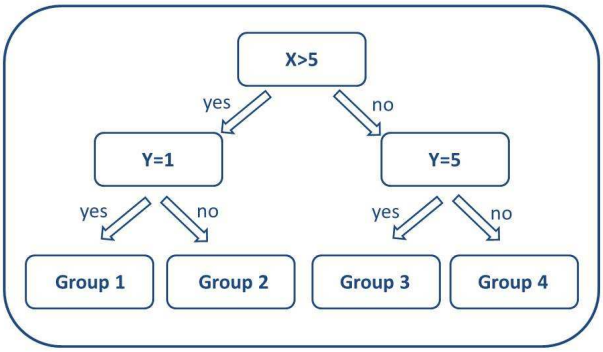

Fig. 4 An example of decision tree

In this scheme calculated descriptors are presented as decision rules. After calculations, every important descriptor can be extracted from random forest and importance (significance) of every descriptor is calculated[52].

Results and discussions

Model development

At the initial preparatory step, a number of descriptors were generated. Then, non-significant, constant descriptors and descriptors with high cross-correlation ($r > 0.90$) were eliminated (one of two descriptors with cross-correlation). In RF approach the model fitting is performed by separate trees which are then combined to a final consensus model. Within each tree the highly correlated descriptors are avoided.

The initial datasets were splitted into training and test sets. Values of toxicity for both test-systems were clusterized by their activity to three groups. The splitting of the dataset to training and test sets (for both *HaCaT* cells and *E.coli* sets) was the same for both cases and fulfill two conditions: 1) metal oxides from each activity group should be presented in both training and test sets; 2) metal oxides presented in test set should cover all types of oxides (MeO, Me_2O_3, MeO_2), similarly to training set. The splitting of data to training and test sets is displayed in Table 1.

Nanoscale Accepted Manuscript

This journal is © The Royal Society of Chemistry [year]

Table 1. Nanoparticle Size, Aggregation, and Toxicity data for both *E.coli* and *HaCaT* toxicity cases

Metal oxide nanoparticle	*E. coli*, log(1/EC_{50})	*HaCaT* cells, log(1/LC_{50})	Size, nm	Aggregation size, nm	Set
Al_2O_3	2.49	1.85	44	372	training
Bi_2O_3	2.82	2.5	90	2029	training
CoO	3.51	2.83	100	257	test
Cr_2O_3	2.51	2.3	60	617	training
Fe_2O_3	2.29	2.05	32	298	training
In_2O_3	2.81	2.92	30	224	training
La_2O_3	2.87	2.87	46	673	training
NiO	3.45	2.49	30	291	training
Sb_2O_3	2.64	2.31	20	223	test
SiO_2	2.2	2.12	150	640	training
SnO_2	2.01	2.67	15	810	training
TiO_2	1.74	1.76	46	265	training
V_2O_3	3.14	2.24	15	1307	training
WO_3	-	2.56	50	180	training
Y_2O_3	2.87	2.21	38	1223	training
ZnO	3.45	3.32	71	189	training
ZrO_2	2.15	2.02	47	661	test

Then, QSAR tasks were processed using Random Forests regression (5 trees, 3 descriptors in each). The statistical fit of a QSAR model was assessed by correlation coefficient r^2 and root-mean-square error of prediction RMSE. The resultant models are characterized with adequate statistical parameters and do possess a good predicting ability. Table 2 summarizes statistical results for both endpoints.

Table 2. Statistical characteristics of RF models

	HaCaT cells	*E.coli*
r^2 (training set)	0.96	0.93
RMSE (training set)	0.10	0.13
r^2 (test set)	0.92	0.78
RMSE (test set)	0.12	0.32

Specifications of developed models (predicted values, standard deviation data, plots of experimentally determined versus predicted values) are presented in Supplementary information.

Model interpretation and comparative analysis

As a result of RF modeling we obtained 6 significant descriptors for *HaCaT* keratinocytes and 7 descriptors for *E.coli*. Absolute impacts for each rule are presented in %. Descriptors S_1, r_w, ρ are the same for both models.

List of important descriptors to *HaCaT* cell cytotoxicity:

S_1 – unbonded two-atomic fragments $[Me]\cdots\cdots[Me]$, which were encoded based on SiRMS-derived descriptors, describing distance where potential reaches minimum at van-der-Waals interactions (43%);

r_w – Wigner-Seitz radius of oxide's molecule (24%);

ρ – mass density (6 %);

(CI) – covalent index of the metal ion (10%);

S_2 – SiRMS-derived number of oxygen's atoms in a molecule, which was described by their electronegativity (15%);

(AP) – aggregation parameter (2%).

List of important descriptors to *E.coli* cytotoxicity:

S_1 – unbonded two-atomic fragments $[Me]\cdots\cdots[Me]$, which was encoded based on SiRMS-derived descriptors, encoding distance where potential reaches minimum at van-der-Waals interactions (7%);

r_w – Wigner-Seitz radius (22%);

ρ – mass density (2%);

(CPP) – cation polarizing power (30 %);

S_2 – SiRMS-derived electronegativity aligned [13] descriptor of oxides molecules – in a sense of the acid-base property of oxides. This parameter increases with a number of oxygens in molecule (3%);

S_3 – tri-atomic fragments $[Me]-[O]-[Me]$, which were encoded by SiRMS-derived descriptors, encoding electronegativity (29%);

(SV) – proportion of surface molecules to molecules in volume (7%).

To generalize classification of developed models all descriptors were combined into four groups: metal-ligand binding characteristics, LDM-based descriptors, SiRMS-based electronegativity's descriptors and SiRMS-based van-der-Waals interactions' descriptors.

The relative contributions of various descriptors (in %) based on decision rules are presented in Figure 5 (*HaCaT* cells) and Figure 6 (*E.coli*).

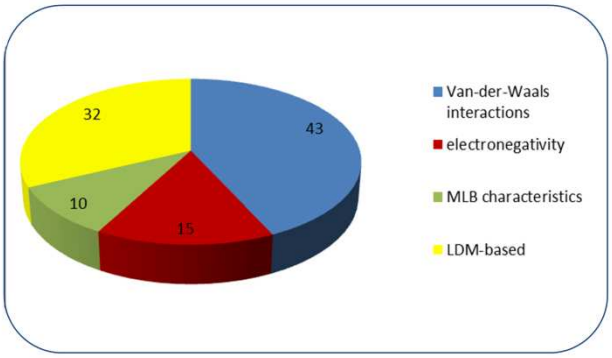

Fig.5 Diagram of relative contribution (in %) of certain descriptors to toxicity (*HaCaT cells)*

Let's take a look at developed models closely. As it can be seen from Fig. 4 and Fig. 5, only contribution sizes of LDM-based descriptors (32% and 31%) are approximately equal in both cases. However, different contributions of other structural parameters in both cases suggest that nanoparticles show different mechanisms of toxicity towards *HaCaT* and *E.coli*.

It is important to note that the Wigner-Seitz radius for both models has close values: 24% for *HaCaT* cells and 22% for *E.coli*. Most probably, Wigner-Seitz radius can describe availability fraction of free molecules on the nanocluster's surface, which actually could be responsible for cytotoxicity.

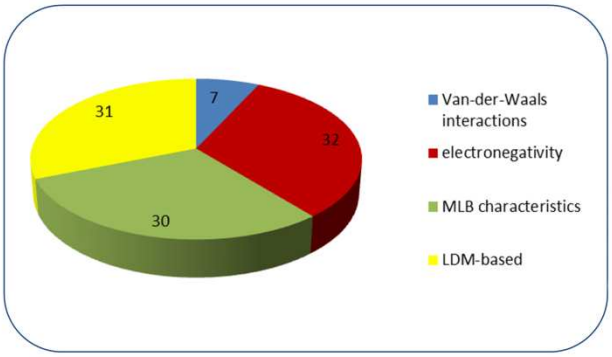

Nanoscale Accepted Manuscript

Fig. 6 Diagram of relative contribution (in %) of certain descriptors to toxicity (*E.coli cells*)

Both models involve a descriptor (ρ) that encodes a mass density, which is one of fundamental properties in LDM (6% for *HaCaT* cells and 2% for *E.coli*). In addition, the developed model for *E.coli* contains a descriptor (*SV*) which reflects a ratio of surface molecules to molecules in volume and has the contribution to the toxicity *ca* 7%. We assume that the difference between contributions of the mass density descriptors in both cells arises from varied interactions of nanoparticle surface with these cells. Also, we suppose, since *HaCaT* cells as eukaryotic cells (about 100nm) are much larger than *E.coli* bacteria cells (about 2nm), the interaction surface is larger for *HaCaT* cell and therefore the contribution of these kinds of descriptors is higher for eukaryotic cells.

Several studies suggest that the mechanism of metal oxide nanoparticles' toxicity depends on release of ions from the surface[45]. Nanoparticles are characterized by a large surface area and it correlates with a high number of reactive surface molecules. Larger number of surface molecules contributes to massive oxidizing capabilities[54]. Earlier, it was suggested that nanoparticles can produce oxidative stress by generation of $O_2^{\bullet-}$ and $^{\bullet}OH$ radicals, so-called reactive oxygen species (ROS):

$$O_2 \longrightarrow O_2^{\bullet-} \quad (8)$$

$$O_2^{\bullet-} + H_2O_2 \longrightarrow {}^{\bullet}OH + OH^- + O_2 \quad (9)$$

Nevertheless the straight link between ROS levels and the induction of toxic effects for different cell types is not explicitly proven yet, but most of the studies support that hypothesis.

In addition, size-dependent LDM-based descriptors may also indirectly describe another mechanism of toxicity. Since in some cases nanoparticles are smaller than cells or cellular organelles, it allows them to penetrate into these main biological systems, disrupting their normal function[3,5,46]. This mechanism links damage of organelles with size of nanoparticles.

According to values of LDM-based descriptors for *E.coli* case it is possible to assume that nanoparticles with larger values of Wigner-Seitz radius (smaller number of molecules present in general nanocluster's volume) exhibit higher toxicity.

Van-der-Waals interactions (S_1) have a high impact in model of toxicity to *HaCaT* cells (43%). In contrast to this, contribution of van-der-Waals interactions to *E.coli* toxicity is considerably smaller (7%). This parameter is responsible for the number of contacts (interactions) between the molecules on surface and those that leave the surface and possibly interacts later with a cell. Therefore, this can contribute to transport of molecule (or cation) to the media or periplasmatic space in the cells. Since eukaryotic cells are capable of internationalizing MOx nanoparticles much easier, the process of detachment from the surface may occur inside the cell. This mechanism is in agreement with the second mechanism of toxicity cased by nano metal oxides explained in our recent study[49]. The difference in contributions of vdW descriptor also could be explained by considerably large difference in cell sizes for both considered cell systems. It seems that larger number of unbounded metal oxide molecules interact per cell in case of eukaryotic cells, i.e. *HaCaT* cells.

Descriptors S_2 are different in both models, but have high correlation. It means that there is a possibility to compare impacts of these descriptors. In case of *HaCaT* cells the value of this descriptor has relatively high impact (15%), comparing with *E.coli* (3%). As these descriptors are related to a number of oxygen's atoms in a molecule, the smaller electronegativity impact is linked to higher toxicity. This parameter characterizes acid-base properties of oxides and increases with a number of oxygens in a molecule. Descriptor S_3 also represents the electronegativity in case of *E.coli* toxicity and has high impact (29%). Thus, the contribution of whole electronegativity is about twice as large for *E.coli* (32%), comparing with *HaCaT* cells (15%).

Descriptors of MLB characteristics for the *HaCaT* cells and *E.coli* toxicity are different. Covalent index (10%) in a model of toxicity to *HaCaT* cells reflects the interaction with protein-bound sulfhydryl's and depleting of glutathione[37]. Cation polarization power (30%) in a model of toxicity to *E.coli* reflects electrostatic interactions[37] and also this comes in agreement with the prevailing impact of SiRMS descriptors, which reflects electronegativity.

The overall schematic representation of suggested mechanisms are showed in Figure 7 (for *HaCaT* cell) and in Figure 8 (for *E.coli* cell).

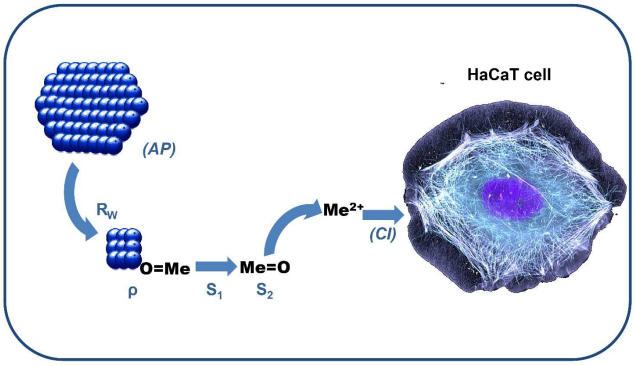

Fig. 7 Schematic representation of the mechanism of metal oxide nanoparticle toxicity for *HaCaT* cell

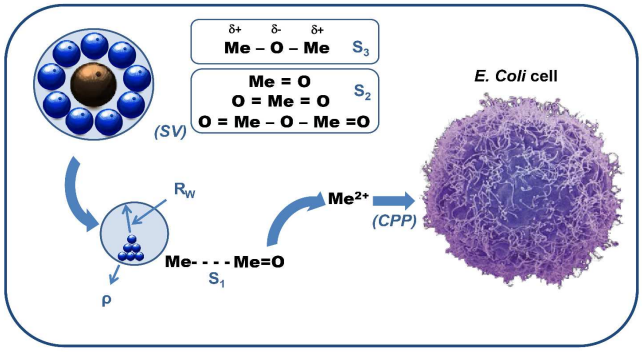

Fig. 8 Schematic representation of the mechanism of metal oxide nanoparticle toxicity for *E.coli* cell

Conclusions

In the present study we combined the analysis of two different experimental toxicity data of metal oxide nanoparticles to *E.coli* cells and *HaCaT* cells. We have utilized a computational modeling methodology to build classification models for quick predictions and to find the difference in contributions of various properties to

Nanoscale Accepted Manuscript

This journal is © The Royal Society of Chemistry [year]

each type of toxicity (*E.coli* or *HaCaT*). The developed nano-QSAR models were validated and reliably predict toxicity for all studied metal oxide nanoparticles. Based on the comparative analysis of properties' contribution in both nano-QSAR models we have found that LDM-based descriptors have almost similar level of contributions to toxicity in both cases, while other parameters (van-der-Waals interactions, electronegativity and metal-ligand binding characteristics) have different contribution levels. Thus, the developed nano-QSAR models reveal the differences in the mechanisms of toxicity of metal oxide nanoparticles to bacteria and a human keratinocyte cell line, which belong to prokaryotic and eukaryotic systems, respectively.

Acknowledgements

The authors thank for support of the NSF CREST Interdisciplinary Nanotoxicity Center NSF-CREST - Grant # HRD-0833178; NSF-EPSCoR Award Number: 362492-190200-01\NSFEPS-0903787. The research leading to these results has received funding from the European Union Seventh Framework Programme (FP7/2007-2013) under Grant Agreement N309837 (NanoPUZZLES project). Also authors are grateful for the financial support of the European Commission through Marie Curie IRSES program, NanoBRIDGES project (FP7-PEOPLE-2011-IRSES, Grant Agreement Number 295128). This work was partially funded by Foundation for the Polish Science within FOCUS program.

Notes and references

[a]*I.I.Mechnikov Odessa National University, Department of Chemistry, Dvoryanskaya str., 2, 65082, Odessa, Ukraine*
[b]*Interdisciplinary Center for Nanotoxicity, Department of Chemistry and Biochemistry, Jackson State University, 1400 J. R. Lynch Street, P. O. Box 17910, Jackson, MS 39217, USA*
[c]*Laboratory of Environmental Chemometrics, Faculty of Chemistry, University of Gdansk, Wita Stwosza 64, 80-308 Gdansk, Poland*
[d]*A.V. Bogatsky Physical–Chemical Institute National Academy of Sciences of Ukraine, 65080, Odessa, Ukraine*

1. *The Global Market for Metal Oxide Nanoparticles to 2020*, Research and Markets, Report, Dublin, Ireland, 2013.
2. J.A. Plant, N. Voulvoulis, K.V. Ragnarsdottir, *Pollutants, Human Health and the Environment: A Risk Based*, 2012.
3. M.C. Garnett, in *Nanonotoxicology: Characterization, dosing and health effects*, eds. N. Monteiro-Riviere and C. Tran, New York, 2007.
4. M. Horie and K. Fujita, in *Advances in Molecular Toxicology*, ed. J. C. Fishbein, Elsevier B.V., Oxford, 2011, vol. 5, pp. 145-178.
5. A. M. Schrand, M. F. Rahman, S. M. Hussain, J. J. Schlager, D. A. Smith and A. F. Syed, *WIREs Nanomed. Nanobiotechnol.*, 2010, **2**, 544-568.
6. T. Puzyn, B. Rasulev, A. Gajewicz, X. Hu, T. P. Dasari, A. Michalkova, H.-M. Hwang, A. Toropov, D. Leszczynska and J. Leszczynski, *Nat. Nanotech.*, 2011, **6**, 175-178.
7. D. Fourches, D. Pu, C. Tassa, R. Weissleder, S. Y. Shaw, R. J. Mumper and A. Tropsha, *ACS Nano*, 2010, **4**, 5703-5712.
8. A. Gajewicz, T. Puzyn, B. Rasulev, D. Leszczynska and J. Leszczynski, *Nanosci. Nanotech. Asia*, 2011, **1**, 53-58.
9. A. Simon-Deckers, S. Loo, M. Mayne-L'hermite, N. Herlin-Boime, N. Menguy, C. Reynaud, B. Gouget and M. Carrière, *Environ. Sci. Technol.*, 2009, **43**, 8423-8429.
10. A. A. Toropov, D. Leszczynska and J. Leszczynski, *Mater. Lett.*, 2007, **61**, 4777-4780.
11. A. A. Toropov and J. Leszczynski, *Chem. Phys. Lett.*, 2006, **433**, 125-129.
12. T. Xia, M. Kovochich, M. Liong, L. Madler, B. Gilbert, H. B. Shi, J. I. Yeh, J. I. Zink and A. E. Nel, *ACS Nano*, 2008, **2**, 2121-2134.
13. X.-R. Xia, N. A. Monteiro-Riviere and J. E. Riviere, *Nature Nanotech.*, 2010, **5**, 671–675.
14. A. Gajewicz, B. Rasulev, T. Dinadayalane, P. Urbaszek, T. Puzyn, D. Leszczynska and J. Leszczynski, *Advanced Drug Delivery Reviews*, 2012, **64**, 1663–1693.
15. A. Poater, A. G. Saliner, M. Sol, L. Cavallo and A. P. Worth, *Expert Opinion on Drug Delivery*, 2010, **7**, 295-305.
16. E. Burello and A. Worth, *Nanotoxicology*, 2011, **5**, 228-235.
17. E. Burello and A. Worth, in *Towards Efficient Designing of Safe Nanomaterials: Innovative Merge of Computational Approaches and Experimental Techniques* eds. J. Leszczynski and T. Puzyn, Royal Society of Chemistry, 2012.
18. H. Zhang, Z. Ji, T. Xia, H. Meng, C. Low-Kam, R. Liu, S. Pokhrel, S. Lin, X. Wang, Y.-P. Liao, M. Wang, L. Li, R. Rallo, R. Damoiseaux, D. Telesca, L. Mädler, Y. Cohen, J. I. Zink and A. E. Nel, *ACS Nano*, 2012, **6**, 4349–4368.
19. G. P. Rivera, G. Oberdörster, A. Elder, V. Puntes and W. J. Parak, *ACS Nano*, 2010, **4**, 5527-5531.
20. T. Puzyn, D. Leszczynska and J. Leszczynski, *Small*, 2009, **5**, 2494-2509.
21. K. Donaldson and V. Stone, *Ann. Ist. Super. Sanita*, 2003, **39**, 405-410.
22. R. Duffin, L. Tran, D. Brown, V. Stone and K. Donaldson, *Inhal. Toxicol.*, 2007, **19**, 849-856.
23. B. Fadeel and A. E. Garcia-Bennett, *Adv. Drug Deliver. Rev.*, 2010, **62**, 362-374.
24. H. K. Lindberg, G. C. M. Falck, S. Suhonen, M. Vippola, E. Vanhala, J. Catalán, K. Savolainen and H. Norppa, *Toxicol. Lett.*, 2009, **186**, 166-173.
25. N. Lubick, *Environ. Sci. Technol.*, 2008, **42**, 8617.
26. M. Lundqvist, *Proc. Natl. Acad. Sci. USA*, 2008, **105**, 14265–14270.
27. A. Magrez, S. Kasas, V. Salicio, N. Pasquier, J. W. Seo, M. Celio, S. Catsicas, B. Schwaller and L. Forro, *Nano Lett.*, 2006, **6**, 1121-1125.
28. A. Nel, T. Xia, L. Madler and N. Li, *Science*, 2006, **311**, 622-627.
29. E. Oberdörster, *Environ. Health Perspect.*, 2004, **112**, 1058-1062.
30. A. E. Nel, L. Mädler, D. Velegol, T. Xia, E. M. V. Hoek, P. Somasundaran, F. Klaessig, V. Castranova and M. Thompson, *Nat. Mater.*, 2009, **8**, 543-557.
31. Marvin 6.1.3, 2013, ChemAxon, www.chemaxon.com
32. DRAGON (Software for Molecular Descriptors Calculation), http://www.talete.mi.it, Version 6.0 edn., 2013.
33. C. Steinbeck, C. Hoppe, S. Kuhn, M. Floris, R. Guha and E. L. Willighagen, *Curr. Pharm. Des.*, 2006, **12**, 2111-2120.
34. Victor E. Kuz'min, A.G. Artemenko, E.N. Muratov, P.G. Polischuk, L.N. Ognichenko, A.V. Liahovsky, A.I. Hromov, E.V. Varlamova, In: *Challenges and Advances in Computational Chemistry and Physics*, Eds: T. Puzyn, J. Leszczynski, Mark T. Cronin, 2010, **8**, 127-176.
35. L. Ahmed, B. Rasulev, M. Turabekova, D. Leszczynska, J. Leszczynski, *Org. Biomol. Chem.*, 2013, **11**, 5798–5808.
36. E. Muratov, A.G. Artemenko, V.E. Kuz'min, N.N. Muratov, E.V. Varlamova, A.V. Kuz'mina, L.G. Gorb, A. Golius, F.C. Hill, J. Leszczynski, A. Tropsha, *SAR QSAR Environ. Res.*, 2011, **22**, 575-601.
37. T. C. Dinadayalane and J. Leszczynski, in *Handbook of Computational Chemistry*, ed. J. Leszczynski, Springer, Heidelberg 2012, pp. 793-867.
38. T. Petrova, B. F. Rasulev, A. A. Toropov, D. Leszczynska and J. Leszczynski, *J. Nanopart. Res.*, 2011, **13**, 3235-3247
39. B. Rasulev, A. Toropov, T. Puzyn, D. Leszczynska, J. Leszczynski, An Application of Graphs of Atomic Orbitals for QSAR Modeling of Toxicity of Metal Oxides, Federation of Analytical Chemistry and Spectroscopy Symposium (FACSS), 2007.
40. A. A. Toropov, D. Leszczynska and J. Leszczynski, *Comput. Biol. Chem.*, 2007, **31**, 127-128.
41. A. A. Toropov, B. F. Rasulev, D. Leszczynska and J. Leszczynski, *Chem. Phys. Lett.*, 2007, **444**, 209-214.
42. A. A. Toropov, B. F. Rasulev, D. Leszczynska and J. Leszczynski, *Chem. Phys. Lett.*, 2008, **457**, 332-336.
43. M. A. Turabekova, B. F. Rasulev, F. N. Dzhakhangirov, D. Leszczynska, J. Leszczynski, *Eur. J. Med. Chem.*, 2010, **45**, 3885-3894.
44. Smirnov B M., *Phys. Usp*, 2011, **54**, 691–721.
45. P. Somasundaran, X. Fang, S. Ponnurangam and B. Li, *KONA Powder Part. J.*, 2010, **28**, 38-49.
46. A. P. Mathews, *Am. J. Physiol.*, 1904, **10**, 290—323

Nanoscale Accepted Manuscript

47. Tatara and e. al, *Aquat. Toxicol.*, 1998, **42**, 255–269.
48. M. C. Newman and e. al, *Environ. Health Persp.*, 1998, **106**, 1419–1425.
49. A. Gajewicz, N. M. Schaeublin, B. Rasulev, S. M. Hussain, D. Leszczynska, T. Puzyn, J. Leszczynski, *Nanotoxicology*, 2014, DOI: 10.3109/17435390.2014.930195.
50. E. Wigner and F. Seitz, *Phys. Rev.* , 1933, **43**, 804–810.
51. V. K. Sharma, *J. Environ. Sci. Health A Tox. Hazard. Subst. Environ. Eng.*, 2009, **14**, 1485-1495.
52. P. G. Polishchuk and e. al, *J. Chem. Inf. Model.*, 2009, **49**, 2481–2488.
53. L. Breiman, *Mach. Learn.*, 2001, **45**, 5–32.
54. Y.-N. Chang and e. al, *Materials*, 2012, **5**, 2850-2871.

Nanoscale Accepted Manuscript

This journal is © The Royal Society of Chemistry [year]